

MacDonald, J. M. , John, C. M. and Girard, J.-P. (2018) Testing clumped isotopes as a reservoir characterization tool: a comparison with fluid inclusions in a dolomitized sedimentary carbonate reservoir buried to 2-4 km. In: Lawson, M., Formolo, M.J. and Eiler, J.M. (eds.) *From Source to Seep: Geochemical Applications in Hydrocarbon Systems*. Series: Geological Society, London, Special Publications (468). Geological Society of London, pp. 189-202. (doi:[10.1144/SP468.7](https://doi.org/10.1144/SP468.7))

This is the author's final accepted version.

There may be differences between this version and the published version. You are advised to consult the publisher's version if you wish to cite from it.

<http://eprints.gla.ac.uk/120399/>

Deposited on: 28 June 2016

1 **Testing clumped isotopes as a reservoir characterisation tool: a comparison with fluid inclusions in**
2 **a dolomitised sedimentary carbonate reservoir buried to 2-4 km**

3
4 John M. MacDonald^{1*}, Cédric M. John¹ & Jean-Pierre Girard²

5
6 ¹Carbonate Research Group, Dept. Earth Science and Engineering, Imperial College London, SW7 2AZ

7 ²TOTAL, CSTJF, Ave Larribau, 64018 Pau

8 *present address: School of Geographical & Earth Sciences, University of Glasgow, G12 8QQ

9 Corresponding address: John.MacDonald.3@glasgow.ac.uk

10
11 **Abstract**

12
13 Constraining basin thermal history is a key part of reservoir characterisation in carbonate
14 rocks. Conventional palaeothermometric approaches cannot always be used: fluid inclusions may be
15 reset or not present while $\delta^{18}\text{O}$ palaeothermometry requires an assumption on the parent fluid
16 composition. The clumped isotope palaeothermometer, however, is a promising technique for
17 constraining the thermal history of basins. In this study we test if clumped isotopes record
18 temperatures of recrystallisation in deeply-buried dolomitic reservoirs, through comparison with
19 fluid inclusion data. The studied reservoir is the Cretaceous Pinda Formation, offshore Angola, a
20 deeply-buried dolomitised sedimentary carbonate hydrocarbon reservoir. It provides an ideal test
21 case as samples from industry wells are available over a relatively wide burial depth range of ~2000-
22 4000 metres below sea floor (mbsf) and the constituent dolomites are relatively homogeneous.

23 Across this depth range, fluid inclusion homogenisation temperatures for the Pinda
24 Formation record a range of temperatures from ~110-170 °C, increasing with depth. These closely
25 match present-day ambient well temperatures, indicating recent resetting of the fluid inclusions.
26 Clumped isotopes, however, record temperatures significantly (~20-60 °C) below fluid inclusion and
27 well temperatures for the seven samples analysed. The deepest five samples (~2800-3700 mbsf)
28 record clumped isotope temperatures around 100-120 °C, interpreted to represent a deep burial
29 recrystallisation event responsible for a massive (re)dolomitisation of the reservoir. The lower
30 clumped isotope temperatures (65 and 82 °C) of the shallower (2055 and 2740 mbsf) samples are
31 interpreted to represent physical mixing of two dolomite generations due to incomplete burial
32 recrystallisation of an early shallow dolomite. Determination of temperature through clumped
33 isotopes allows calculation of the parent fluid $\delta^{18}\text{O}$ values. In the five deepest samples, the fluid $\delta^{18}\text{O}$
34 values of 3.7-6.5 ‰ cluster around the modern-day porewater composition (5 ‰) suggesting burial
35 dolomitisation occurred in the presence of evolved brine. Mineral $\delta^{18}\text{O}$ values of ~-4.5 to -7 ‰ are
36 lower than pristine Cretaceous marine dolomite and are in accordance with burial recrystallisation.
37 Clumped isotopes are therefore interpreted to record temperatures corresponding to open-system
38 burial recrystallisation events. This study shows that clumped isotopes are a valuable tool in
39 characterising the thermal history of deeply-buried (>2000 m) carbonate hydrocarbon reservoirs.

40
41 Keywords: clumped isotopes; dolomite; recrystallisation; $\delta^{18}\text{O}$; palaeothermometry

42
43 **Introduction**

45 A key aspect in understanding the history of hydrocarbon reservoirs is to characterise their
46 thermal history. Indeed, thermal exposure is known to be a prime factor in the degradation of
47 hydrocarbon reservoirs (e.g. Nadeau, 2011). Changing temperature, for example during burial, can
48 cause diagenetic recrystallisation which may affect physical reservoir characteristics such as porosity
49 and permeability, and impact hydrocarbon recovery rates. The thermal history also affects
50 hydrocarbon maturation. In basins containing carbonate rocks, the two main approaches to
51 characterising thermal history in rocks of all ages are fluid inclusion (e.g. McLimans, 1987; Barker &
52 Goldstein, 1990; Goldstein, 2001) and $\delta^{18}\text{O}$ (McCrea, 1950; Epstein, *et al.*, 1951)
53 palaeothermometry. These techniques are well-established but have some drawbacks which may
54 limit their application. Fluid inclusion palaeothermometry can be used to infer burial temperatures,
55 and hence potentially burial recrystallisation, by measuring homogenisation temperature (T_h). This is
56 obtained by heating a two-phase inclusion until the vapour bubble disappears and all that remains is
57 a single-phase liquid (e.g. Goldstein & Reynolds, 1994). However, two-phase fluid inclusions are not
58 always present or may not be large enough to reliably measure. This severely limits their use as a
59 palaeothermometer in fine-grained carbonates. In addition, in the context of basin evolution,
60 perhaps the most significant drawback is that they may stretch during subsequent burial, resulting in
61 a resetting of T_h temperatures at present-day temperatures (e.g. Goldstein & Reynolds, 1994). This
62 leads to fluid inclusions recording maximum burial temperatures, i.e. a temperature higher than the
63 temperature at which the host mineral precipitated or recrystallized.

64 The $\delta^{18}\text{O}$ palaeothermometer is based on the relationship between mineral $\delta^{18}\text{O}$,
65 temperature and the $\delta^{18}\text{O}$ of the parent fluid from which the mineral formed (McCrea, 1950;
66 Epstein, *et al.*, 1951). Measuring $\delta^{18}\text{O}$ in carbonates has been routine for many decades (e.g. Urey, *et al.*,
67 1951; Emiliani, 1955; Shackleton, 1967) but in order to calculate temperature, the $\delta^{18}\text{O}$ of the
68 parent fluid must be known. In most cases this value is unconstrained and an assumption must be
69 made. An incorrect assumption by only 1 ‰ may lead to a temperature estimate greater than ten
70 degrees away from the true mineral formation temperature.

71 Clumped isotopes is a promising method which avoids the pitfalls in these other
72 palaeothermometers. This technique is based on the thermodynamic relationship between
73 carbonate mineral growth temperature and the abundance of chemical bonding (“clumping”)
74 between ^{13}C and ^{18}O isotopes (expressed as Δ_{47}) within single carbonate ions (e.g. Ghosh, *et al.*,
75 2006a; Schauble, *et al.*, 2006; Eiler, 2007). This relationship has led to the application of the
76 carbonate clumped isotope palaeothermometer to address a range of geological questions. Most
77 studies have focussed on surface and near-surface applications where the temperatures involved
78 are in the ~0-35 °C range, including palaeoclimate (e.g. Affek, *et al.*, 2008; Passey, *et al.*, 2010;
79 Thiagarajan, *et al.*, 2014) and palaeoaltimetry (e.g. Ghosh, *et al.*, 2006b; Huntington, *et al.*, 2010;
80 Lechler, *et al.*, 2013; Carrapa, *et al.*, 2014) studies. The carbonate clumped isotope
81 palaeothermometer can also be applied in the ~50-300 °C range, relevant to processes such as
82 diagenesis and dolomitisation (Ferry, *et al.*, 2011; Passey & Henkes, 2012; MacDonald, *et al.*, 2013;
83 Dale, *et al.*, 2014; Henkes, *et al.*, 2014; Sena, *et al.*, 2014; Vandeginste, *et al.*, 2014; Geske, *et al.*,
84 2015; John, 2015; Kluge & John, 2015; Kluge, *et al.*, 2015; MacDonald, *et al.*, 2015; Shenton, *et al.*,
85 2015; Stolper & Eiler, 2016).

86 The ability of carbonate clumped isotopes to retain temperatures of original precipitation or
87 fluid-driven recrystallisation at burial temperatures of 50-300 °C is not well established yet. Burial of
88 carbonate rocks may lead to open-system recrystallisation, whereby pre-existing carbonate minerals
89 dissolve on contact with a fluid and reprecipitate. Assuming complete open-system recrystallisation,

90 the Δ_{47} value should reflect the ambient temperature during recrystallisation. However, recent work
91 (Dennis & Schrag, 2010; Passey & Henkes, 2012; Henkes, et al., 2014) has suggested that
92 temperatures attained during burial may lead to closed-system resetting of clumped isotopes, where
93 intra-crystal diffusion of O and C occurs and Δ_{47} does not necessarily record the temperature at
94 which open-system recrystallisation occurred but is locked at a temperature between formation
95 temperature and the maximum temperature of burial. Clumped isotope measurements of pristine
96 carbonatites have given a wide range of temperatures, many around ~150-250 °C, which are
97 interpreted as blocking temperatures during cooling (Dennis & Schrag, 2010). Without
98 recrystallisation during burial diagenesis, the mechanism proposed for attaining the cooling
99 temperatures is solid-state closed-system bond reordering of C-O bonds in the carbonate lattice
100 (Dennis & Schrag, 2010; Passey & Henkes, 2012). If calcite is exposed to temperatures greater than
101 ~100 °C for millions of years, bond reordering may occur (Dennis & Schrag, 2010; Passey & Henkes,
102 2012; Henkes, et al., 2014; Stolper & Eiler, 2015), bringing the clumped isotope temperatures to the
103 ambient temperature.

104 The fact that bond reordering can occur in calcite held at >100 °C for millions of years
105 indicates that it is a key process to consider when investigating the utility of clumped isotopes in the
106 characterisation of deeply-buried reservoirs. Studies on bond reordering have concentrated on
107 calcite while in this study we focus on a dolomitic reservoir. The only available kinetics data on bond
108 reordering in dolomite is from a published conference abstract by Bonifacie et al., (2013); this
109 suggested unpublished experimental data indicated dolomite was resistant to solid-state bond
110 reordering up to ~300 °C. This suggests that bond reordering will have a lesser effect, if any, on the
111 preservation of temperature signatures recorded by clumped isotopes in dolomite. In this study, we
112 compare clumped isotope temperatures with an extensive suite of previously acquired fluid
113 inclusion and ambient well temperatures (Walgenwitz, *et al.*, 1990; Eichenseer, *et al.*, 1999) to
114 investigate if clumped isotopes in dolomite are affected by bond reordering, or whether they are
115 recording temperatures of geologically meaningful events such as burial recrystallisation.

116

117 **Sample Characterisation**

118 *Geological Setting*

119 The dolostone samples investigated in this study are from the Cretaceous Pinda dolomite
120 Formation from offshore Angola (Fig. 1a). The tectonic framework of the Pinda Formation begins
121 with the breakup of southwestern Gondwana during the Early Cretaceous (Reyre, 1984). The initial
122 rifting phase and associated sedimentary deposition was dominated by lacustrine sediments
123 (Eichenseer, et al., 1999), followed by evaporite formation (e.g. Coajou & Ribeiro, 1994). As
124 continental rifting continued northwards, marine transgression took place and marine carbonates of
125 the Pinda Formation were deposited during Albian time (Koutsoukos, *et al.*, 1991). Halokinesis
126 during the Albian resulted in turtle-back and raft structures which created hydrocarbon traps
127 (Bremner, *et al.*, 1993; Eichenseer, et al., 1999).

128 Modelling of the burial history of the Pinda Formation by TOTAL indicates that after
129 deposition of the thick Pinda sequence, there was little or no burial until the Oligocene (Fig. 1b). This
130 is supported by Walgenwitz et al., (1990) who indicated that diagenesis mainly took place in the
131 late Oligocene following reactivated subsidence. Initial dolomitisation of the Pinda carbonates is
132 interpreted to have occurred during early diagenesis, producing dolomite microrhombs (Eichenseer,
133 et al., 1999). Early dolomitisation was amplified by later shallow burial recrystallisation, producing
134 cloudy dolosparites with a clear outer rim (Eichenseer, et al., 1999). It was proposed that this later

135 recrystallisation was triggered by mixed saline-meteoric fluid circulations at shallow depth (mixing-
136 zone dolomitisation) and resulted in a significant modification of the original geochemical signature
137 of the dolostone (Eichenseer, et al., 1999). Eichenseer et al., (1999) indicated no evidence in support
138 of a late deep burial (high temperature) dolomitisation event, and considered that the bulk of the
139 dolomitisation was of early shallow origin. The current model of dolomitisation for the Pinda
140 Formation therefore relies solely on a mixing-zone dolomitisation mechanism, which took place
141 during early diagenetic stages in relation with sea level fall and prior to any significant burial.

142

143 *Fluid Inclusions*

144 Fluid inclusion thermometry was conducted by TOTAL and details of the microthermometric
145 procedures and measurements are given in Walgenwitz et al., (1990). Fluid inclusion measurements
146 were conducted on two-phase fluid inclusions located in crystals of dolosparite and in recrystallized
147 feldspar grains. A large suite of homogenisation temperatures was obtained from ~40 samples
148 across the Pinda Formation in the study area (13 wells). Homogenisation temperatures (T_h) range
149 from ~110 to 170 °C (Fig. 2). The fluid inclusion assemblage exhibits a roughly linear temperature-
150 depth relationship, coincident with a suite of downhole ambient well temperature readings (Fig. 2).
151 This was interpreted by Eichenseer et al., (1999) as reflecting progressive resetting of fluid inclusion
152 T_h values during burial down to present-day depths. However, the error bars on many of these are
153 large and make confident interpretation difficult (see further discussion below). Homogenisation
154 temperatures (sample averages) corresponding to the specific core plug samples selected for
155 clumped isotope analysis range from 111 to 152 °C (Table 1).

156

157 **Clumped Isotopes**

158 *Methodology*

159 Carbonate clumped isotope measurements were carried out in the Qatar Stable Isotope
160 Laboratory at Imperial College London. Samples were powdered using a dental drill. In order to
161 remove hydrocarbons and other organic matter, the powders were treated with 4 to 8 washes in a
162 cold cleaning solution of 3 % H_2O_2 and 0.9 wt% sodium hexametaphosphate. Subsequently the
163 treated powders were washed with ethanol and DI water before being dried in an oven at 50 °C to
164 evaporate any remaining water. Where this treatment was not sufficient, sample powders were
165 treated in a TePla 400 oxygen plasma asher at the London Centre for Nanotechnology at University
166 College London. Powders were placed in petri dishes and heated at ~40 °C for 5 minutes in an
167 oxygen plasma. The method resulted in the complete combustion of all organic matter under
168 vacuum after a 5 minute treatment. Given the short treatment time, the temperature in the oxygen
169 plasma asher only reaches ~40 °C, well below the temperature threshold for initiating closed-system
170 bond reordering. Additionally, this method was tested on a Carrara Marble standard and was not
171 found to have any effect on clumped isotope systematics. For clumped isotope analysis, 5-6 mg of
172 sample powder was reacted under vacuum with 104 % phosphoric acid at 90 °C for 20 minutes.
173 Water generated during the reaction was separated from the produced CO_2 by first trapping in
174 liquid nitrogen then swapping the liquid nitrogen for an ethanol-liquid nitrogen mixture held at ~-90
175 °C. The water remained frozen while the CO_2 was passed through a Poropak Q chromatography trap
176 held at -35 °C. Full details on the purification procedure are described in Dale et al., (2014).

177 The purified CO_2 was measured in one of two Thermo Fisher MAT 253 isotope ratio mass
178 spectrometers (Pinta and Nina, see Supplementary Data) in dual inlet mode with a measurement
179 time of ~2.5 hours. Masses 44-49 were measured, with 48 and 49 used to test for potential

180 contamination as CO₂ with those molecular masses is extremely rare relative to mass 47 (e.g. Eiler,
181 2007). Only samples with δ_{48} and Δ_{48} values that fall within 2 ‰ of the heated gas line (Δ_{48} Offset)
182 and had a 49 Parameter of <0.2 were accepted (Dale, et al., 2014). Mass spectrometer non-linearity
183 was corrected based on methods described in Huntington et al., (2009) using a 30-day moving
184 average of heated gases as this provided a suitable number of heated gases and carbonate
185 standards to correct against. All Δ_{47} values reported are in the Carbon Dioxide Equilibrated Scale
186 (CDES) (Dennis, *et al.*, 2011) using a secondary transfer function based on Carrara Marble, ETH-3 (an
187 externally verified carbonate standard (Iso C in Meckler, *et al.*, 2014)) and heated gases. Following
188 correction to the absolute reference frame, the empirical acid fractionation factor of +0.069 ‰
189 calculated in Guo et al., (2009) and experimentally derived by Wacker et al., (2013) was added to
190 the Δ_{47} value to bring the data into the 25 °C scale used in calibrations. This acid fractionation factor
191 is consistent with internal laboratory tests at Imperial College London, and with the values used for
192 the Imperial College calibration (Kluge et al, 2015). The Carrara Marble standard gave a linearity- and
193 acid-corrected average Δ_{47} value of 0.382 ± 0.020 ‰ across both mass spectrometers while the ETH-3
194 value was 0.700 ± 0.016 ‰; these compare well with published values of 0.395 ‰ (Dennis, et al.,
195 2011) and 0.705 ‰ (Meckler, et al., 2014) respectively. All standard and sample data are given in the
196 Supplementary Data Table. For $\delta^{18}\text{O}_{\text{dolomite}}$, the acid fractionation factor of Rosenbaum and Sheppard
197 (1986) was applied. The calibration of Kluge et al., (2015) was used to convert Δ_{47} into temperature
198 as this is the only experimental calibration that extends over the 25-250 °C range, and it was derived
199 using the same methods and instruments as in this study. $\delta^{18}\text{O}_{\text{porewater}}$ values were calculated with
200 the carbonate-water equilibrium fractionation factors from Land (1980). The calculated $\delta^{18}\text{O}_{\text{porewater}}$
201 are reported in the Vienna Standard Mean Ocean Water (VSMOW) scale, whilst measured $\delta^{18}\text{O}$
202 and $\delta^{13}\text{C}$ values are reported in the Vienna PeeDee Belemnite (VPDB) scale.

203

204 *Results*

205 Seven dolostone bulk samples from six different wells were selected for clumped isotope
206 analysis. The samples were taken from depths ranging from 2055 to 3705 metres below sea floor
207 (mbsf). They are generally unimodal planar-S (Sibley & Gregg, 1987) dolosparites (Fig. 3a); one
208 sample contains very minor calcite (Fig. 3b) and most have isolated quartz grains (Fig. 3a). Crystal
209 size range is ~50-500 μm and shape is anhedral to euhedral. The smallest, most euhedral dolomite
210 rhombs are found lining moldic pores (Fig. 3c) after dissolution of ooids – a fabric commonly
211 preserved (Fig. 3b). Dolomitized shelly fragments are also occasionally observed (Fig. 3d).

212 The $\delta^{13}\text{C}$ values of the seven samples are all within a narrow range of ~3-3.5 ‰ and do not
213 correlate with depth (Fig. 4a, Table 1). $\delta^{18}\text{O}$ values range from ~-3.5 to -7 ‰ (Fig. 4b, Table 1) and do
214 not correlate with depth or $\delta^{13}\text{C}$, although the shallowest sample has the least depleted $\delta^{18}\text{O}$ value.
215 Δ_{47} values range from 0.495 to 0.592 ‰, which translates to temperatures of 65 to 122 °C, with
216 temperature errors in the range of ± 1 to ± 7 °C. Temperatures increase with burial depth in the two
217 shallower samples before clustering around 100-120 °C in the five deeper samples (Fig. 4c, Table 1).
218 The shallowest sample (JM2055) has a calculated parent fluid $\delta^{18}\text{O}$ value of 1.7 ‰, rising to 2.7 ‰ in
219 the next deepest sample (JM2740) (Fig. 4d, Table 1). The five deeper samples, which record clumped
220 isotope temperatures of ~100-120 °C (average = 111 °C), exhibit calculated fluid $\delta^{18}\text{O}$ values of 3.7-
221 6.5 ‰ (average = 4.9 ‰), with no depth trend. These five samples plot within or close to
222 the modern-day porewater $\delta^{18}\text{O}$ of ~5 ‰ (Walgenwitz, 1989).

223

224 **Discussion**

225 Interpretation of the fluid inclusion homogenisation temperatures is complicated by the fact
226 that they have large error bars and record a spread of temperatures of ~110-170 °C, which likely
227 reflects thermal re-equilibration during burial subsequent to fluid inclusion trapping. It is well known
228 that not all fluid inclusions are affected in the same way by thermal resetting, some fluid inclusions
229 being more resistant than others depending on their size and shape (Goldstein, 2001). The lowest T_h
230 values recorded in the fluid inclusions are at ~110 °C (Fig. 2) and would therefore represent the most
231 conservative temperature for any burial dolomitisation episode. Eichenseer et al. (1999) did not
232 interpret any such late burial dolomitisation. The higher T_h values recorded by fluid inclusions up to
233 170 °C in the Pinda Formation reflect a subsequent increase in the ambient temperature and
234 thermal resetting of fluid inclusions without dolomite recrystallisation. Where ambient
235 temperatures were available (five of the seven samples), homogenisation temperatures are within
236 10 °C of the present-day ambient temperature (Fig. 4c, Table 1).

237 Clumped isotope temperatures, however, fall well below present-day ambient well
238 temperatures and average fluid inclusion temperatures at all investigated depths by about 20 to 60
239 °C (Table 1, Fig. 4c). The clumped isotope temperature of ~100-120 °C recorded by the five deeper
240 samples is consistent over a ~1000 m depth range (~2800-3700 mbsf; Fig. 4c) and close to the lower
241 end of the range of fluid inclusion T_h values (~110 °C, Fig. 2). This strongly suggests that the clumped
242 isotopes in these five samples are recording a single open-system recrystallisation event, interpreted
243 to represent a deep burial recrystallisation episode responsible for the blocky planar-s texture
244 observed in the studied samples. The fluid $\delta^{18}\text{O}$ values (~3.5-6.5 ‰) calculated for these samples are
245 clustered around modern-day porewater composition (5 ‰) and suggest consistent brine $\delta^{18}\text{O}$
246 values with the time of burial diagenesis. The similarity between present- and palaeo-fluid
247 compositions is suggestive of open-system recrystallisation (dissolution-reprecipitation). With open-
248 system recrystallisation, the $\delta^{18}\text{O}$ value of the carbonate will reflect the ambient temperature
249 and $\delta^{18}\text{O}$ value of the fluid that enabled recrystallisation to occur. Therefore, if either of these two
250 parameters (ambient temperature or fluid $\delta^{18}\text{O}$) did vary during the open-recrystallisation process
251 then the mineral $\delta^{18}\text{O}$ values should also vary over a depth range in a single formation/basin. This is
252 the case of the five deeper samples of the Pinda Formation investigated in this study which have
253 undergone complete burial recrystallisation and show a 2 ‰ range in their bulk $\delta^{18}\text{O}$ values,
254 reflecting a variation of ~20 °C in temperature and ~2.8 ‰ in fluid $\delta^{18}\text{O}$. Eichenseer et al., (1999)
255 interpreted measured bulk $\delta^{18}\text{O}$ values of these sediments to record isotopic resetting during burial
256 of early seafloor dolomite. Indeed, the mineral $\delta^{18}\text{O}$ values reported by Eichenseer et al., (1999) and
257 in our study are more depleted than typical marine carbonate values from the Cretaceous (Veizer, *et*
258 *al.*, 1999), and cannot reflect early seafloor conditions.

259 After deposition of the ~1-1.5 km-thick Pinda Formation in the Albian, there was little or no
260 burial until the Oligocene (Fig. 1b) when the Pinda sediments were buried under a thick sequence of
261 Oligocene and Miocene sediments, with a steady subsidence continuing to the present day. The
262 base of the Pinda Formation was buried from ~1.4 km at the beginning of the Oligocene to ~2.7 km
263 at the end of the Oligocene, reaching a burial temperature of ~100 °C, based on the present-day
264 geothermal gradient of 40-45 °C/km (Walgenwitz, et al., 1990). According to (Walgenwitz, et al.,
265 1990) a major diagenetic event occurred at ca. 25 Ma, towards the end of the episode of Oligocene
266 subsidence. It therefore seems highly plausible that bulk and clumped isotopes record burial
267 recrystallisation of dolomite during a major diagenetic event at about 100-120°C and at ca. 25 Ma
268 (Fig. 1b).

269 The two shallowest samples (2055 & 2739 mbsf) have clumped isotope temperatures of 65
270 and 82 °C, somewhat lower than the deeper samples. The present-day well temperatures at these
271 shallower depths, 111 °C and 141 °C respectively, are also lower than that of the deeper samples
272 (147-161 °C), and close to the hotter end of the temperature of the later burial dolomitisation
273 episode (~120°C). The clumped isotope temperatures of these samples are therefore best explained
274 as reflecting incomplete dolomite recrystallisation and physical mixing of the two generations of
275 dolomite, i.e. early shallow dolomite (~35 °C) and burial dolomite (~100-120 °C).

276 In all samples, fluid inclusions have been reset to near present-day temperatures while
277 clumped isotopes have not and are instead interpreted to record open-system recrystallisation. This
278 is in accord with previous studies of subsurface carbonates which have suggested recrystallisation
279 temperatures are recorded in clumped isotope systematics. John (2015) found that clumped
280 isotopes were recording deposition and recrystallisation in a suite of Cretaceous oysters from Oman.
281 One well-preserved individual recorded a primary precipitation temperature of 37±4 °C and a fluid
282 $\delta^{18}\text{O}$ value typical of slightly-evaporated Cretaceous seawater in a restricted platform basin. Other
283 oysters from the suite, however, record clumped isotope temperatures of ~60-70 °C indicating at
284 least partial burial recrystallisation. Ferry et al., (2011) calculated clumped isotope temperatures of
285 ~40-80 °C in the Latemar Platform which they attributed to initial dolomitisation while Sena et al.,
286 (2014) used clumped isotopes to show that early dolomite re-equilibrated through neomorphism
287 from proto-dolomite to well-ordered dolomite with fluids at 60-70 °C in a shallow burial setting in a
288 Tethyan carbonate platform in Oman.

289 It is however important to address the potential for closed-system bond reordering (Passey
290 & Henkes, 2012; Henkes, et al., 2014; Stolper & Eiler, 2015) to have occurred. Assuming open-
291 system behaviour, the Δ_{47} value should reflect the ambient temperature during recrystallisation.
292 However, recent work has indicated that closed-system resetting of clumped isotope systematics
293 can occur at high temperatures, thus resetting the Δ_{47} value recorded earlier during deposition or
294 after open-system recrystallisation. If calcite is exposed to temperatures of greater than ~100 °C for
295 tens to hundreds of millions of years, this bond reordering may occur (Dennis & Schrag, 2010; Passey
296 & Henkes, 2012; Henkes, et al., 2014). The reordering process is interpreted to be a two-stage
297 process with initial rapid isotope diffusion resulting in a change of ~1-40 °C at ambient temperatures
298 of ~75-120 °C sustained for ~100 Myr. Following this, slow isotope exchange reactions between
299 adjacent carbonate groups at >~150 °C sustained for >~100 Myr could bring the clumped isotope
300 temperatures to the ambient temperature (Henkes, et al., 2014; Stolper & Eiler, 2015). Such bond
301 reordering in calcite has been documented in natural samples. Dennis and Schrag (2010)
302 hypothesised that some form of closed-system reordering must be occurring during slow cooling of
303 rocks as they found that carbonatites with no petrographic or geochemical evidence for diagenesis
304 were recording clumped isotope temperatures well below those expected for carbonatite
305 crystallisation temperatures. This study led to the initial development of the bond reordering
306 hypothesis, showing that the clumped isotope composition of calcite and phosphate did change in
307 laboratory experiment when these minerals were exposed for several weeks at temperatures in
308 excess of 200 °C (Passey & Henkes, 2012; Henkes, et al., 2014; Stolper & Eiler, 2015). Shenton et al.,
309 (2015) further confirmed with natural samples that different components (brachiopods, crinoids etc)
310 of calcite limestones from the Palmarito Formation, Venezuela, and the Bird Springs Formation,
311 Nevada, were affected by bond reordering during burial (to ~4-5 km, 150-175 °C) and exhumation.

312 The only available constraints on the kinetics of bond reordering in dolomite are from the
313 published conference abstract of Bonifacie et al., (2013) which indicated dolomite was resistant to

314 solid-state bond reordering up to ~ 300 °C. Until the full results of these experiments - and hence the
315 parameters required for modelling closed-system bond reordering in dolomite - are published, the
316 exact effects of bond reordering on the Pinda Formation dolostones cannot be determined. We note
317 that 300 °C is well above the well temperature offshore Angola, where our samples come from but
318 how would the Pinda dolomite behave, if we assumed dolomite had similar Arrhenius parameters to
319 calcite? In the absence of dolomite-specific modelling parameters, we used the bond reordering
320 model for calcite of Passey and Henkes (2012) to investigate a 'worst-case' scenario for bond
321 reordering in the Pinda dolostones. This was conducted using the input parameters for optical
322 calcite MGB-CC-1 (Passey & Henkes, 2012) using their Equation 13 (first-order kinetics) and the
323 evolution of Δ_{47} through time is modelled in the style of the Thermal History Reordering Models of
324 Shenton et al. (2015).

325 Four scenarios were modelled. Three of these use a 'representative' Pinda burial curve,
326 based on the dashed line on Figure 1b from thermal modelling by TOTAL for sample JM2923. These
327 scenarios vary in their diagenetic histories: no post-deposition recrystallisation (scenario 1); shallow
328 dolomitisation only (scenario 2); shallow dolomitisation and burial recrystallisation at ca. 25 Ma at a
329 burial temperature of 115 °C (scenario 3) (Walgenwitz, et al., 1990). Scenario 4 is specific to the base
330 of the Pinda Formation (sample JM3705), using an extrapolation of the representative Pinda curve to
331 the present-day depth of ~ 3.7 km and ambient temperature inferred to be 170 °C from the
332 geothermal gradient (dotted line in Figure 1b). For all 4 scenarios, deposition is assumed to be at 25
333 °C with shallow dolomitisation at 35 °C and burial recrystallisation at 25 Ma, if applicable
334 (Walgenwitz, et al., 1990). For each of the (re)crystallisation events (deposition, early
335 dolomitisation, recrystallisation during burial), the Δ_{47} is controlled by the temperature of the
336 respective process, regardless of whether any change on Δ_{47} due to bond reordering has occurred
337 before, as each represents an open-system (re)precipitation. Modelling results are shown in Figure
338 5.

339 In all four scenarios, no closed-system bond reordering occurs before the end of the
340 Oligocene burial despite the ambient temperature reaching ~ 130 °C in the base Pinda scenario. In
341 scenario 4 (base Pinda), the burial curve indicates that the open-system burial recrystallisation will
342 occur at ~ 130 °C, i.e. towards the end of the Oligocene. As the ambient temperature increases from
343 130 °C to 170 °C in the 25 Myr between recrystallisation and the present-day, the temperature
344 would be high enough to drive the Δ_{47} values in calcite to the ambient temperature resulting in 100
345 % bond reordering (Fig. 5a) and a recorded temperature of 170 °C. With the 'representative' Pinda
346 burial history (sample JM2923, scenario 3), the burial curve indicates that the open-system burial
347 recrystallisation will occur at ~ 115 °C towards the end of the Oligocene (Fig. 5b). As the ambient
348 temperature increases from 115 °C to 147 °C (sample JM2923, Table 1 & Fig. 4c) in the 25 Myr
349 between recrystallisation and the present-day, modelling indicates partial reordering of the Δ_{47}
350 value would occur in calcite to a present-day clumped isotope temperature of 120 °C. Open-system
351 burial recrystallisation at is important in facilitating post-recrystallisation closed-system bond
352 reordering in calcite as in the scenarios where no burial recrystallisation is assumed (scenarios 1 and
353 2), there is very limited bond reordering. With shallow dolomitisation only (scenario 2), bond
354 reordering would modify the observed temperature from 35 to 47 °C and with no post-deposition
355 recrystallisation at all, bond reordering would modify the temperature from 25 to 37 °C (Fig. 5b).

356 Although the temperature generated through partial bond reordering of sample JM2923
357 (scenario 3) is close to the recorded clumped isotope temperature, it must be emphasised that these
358 reordering models are based on the kinetics of calcite. Dolomite is perceived to have much slower

359 reordering kinetics (Bonifacie, et al., 2013). This is emphasised by the fact that modelling of bond
360 reordering using the kinetics for calcite and the burial curve for the base of the Pinda Formation
361 indicates that sample JM3705 would record the present-day ambient temperature of ~170 °C in its
362 clumped isotope systematics. This is not the case – the clumped isotope temperature for this sample
363 is 118 °C, well below ambient temperature (Table 1, Fig. 4c) reflecting the interpreted
364 recrystallisation event at ca. 110 °C. We also note that we used the same Arrhenius parameters for
365 bond reordering in the early dolomite and the recrystallised burial dolomite. This is unlikely to be the
366 case, and recrystallised dolomite could be more resistant to bond reordering as it was equilibrated
367 at higher temperature. The degree of stoichiometry of (proto-)dolomite is also likely to complicate
368 bond reordering models. We acknowledge that while the kinetics of dolomite reordering are
369 unpublished, our interpretation that the Pinda Formation dolostones are recording the temperature
370 of diagenetic events cannot be proven beyond doubt. However, if the conclusions of Bonifacie et al.,
371 (2013) are valid, the temperature conditions (~300 °C) thought to be required for solid-state bond
372 reordering in dolomite were not reached in the studied samples. This is supported by the results of
373 our modelling simulations, that shows that the temperature recorded are compatible with a 110°C
374 recrystallization. Therefore our interpretation that the clumped isotopes are recording burial
375 recrystallisation is well-founded.

376 The specificity of our study in the Pinda formation of offshore Angola is that samples are
377 from deep cores and are at their maximum burial depth in the present day. This enables insight into
378 clumped isotope systematics during deep burial without the complication of any potential closed-
379 system resetting during slow geological exhumation as was encountered by Shenton et al., (2015).
380 We suggest that in the Pinda Formation clumped isotopes are recording the palaeotemperatures of
381 an open-system recrystallisation event that resulted in massive burial dolomitisation of an already
382 dolomitic reservoir. Hence, reasonable fluid $\delta^{18}\text{O}$ values are calculated when using the clumped
383 isotope data, while they appear rather high when using the fluid inclusion homogenisation
384 temperatures. This illustrates that clumped isotope analysis can be a valuable tool in investigating
385 the thermal history of deeply-buried carbonate reservoirs, and that it is of particular interest for
386 distinguishing early-shallow from late-burial dolomitisation processes. In the Pinda Formation
387 dolostones, the clumped isotopes recorded open-system burial recrystallisation at a temperature of
388 ~100-120 °C. Our data further indicate that the clumped isotope signal was preserved during
389 subsequent burial to conditions ~1600 m deeper (~3700 mbsf) and ~50 °C hotter (up to 161 °C).
390 While the clumped isotope geothermometer does not yet have the spatial resolution to interrogate
391 zonation within individual crystals or distinguish between multiple generations of thin cement
392 layers, this study does show that its application to bulk samples has the ability to record diagenetic
393 information in relatively homogeneous monophasic dolostones. It has indicated that the massive
394 blocky planar-s dolosparite in the Pinda Formation formed during late burial recrystallisation at
395 ~100-120 °C, a process that could not be documented from petrography and $\delta^{18}\text{O}$ (Eichenseer, et al.,
396 1999). Advances in methodology (e.g. Hu, *et al.*, 2014; Petersen & Schrag, 2014) to increase spatial
397 resolution to the millimetre and sub-millimetre scale will enable much wider usage of the clumped
398 isotope palaeothermometer in reservoir characterization.

399

400 **Conclusions**

401 This study examined if carbonate clumped isotope palaeothermometry could be applied to
402 characterise the thermal history of dolomitised sedimentary carbonate hydrocarbon reservoirs. It
403 was performed on a set of seven dolostone samples from the Pinda Formation of offshore Angola

404 presently lying at their maximum burial depth, ~2000-3700 mbsf. Clumped isotope data suggest
405 that temperatures derived from a well-established palaeothermometric technique – fluid inclusions
406 – have been reset to current ambient well temperatures. Clumped isotope temperatures, however,
407 record lower temperatures corresponding to open-system burial recrystallisation occurring prior to
408 present-day maximum burial. Fluid $\delta^{18}\text{O}$ values calculated for the five deepest samples overlap with
409 present-day porewater $\delta^{18}\text{O}$ while mineral $\delta^{18}\text{O}$ supports the conclusion that clumped isotopes are
410 recording burial recrystallisation conditions. Closed-system isotopic bond reordering is not believed
411 to have affected the Pinda Formation samples, therefore we contend that clumped isotope analysis
412 can be a valuable tool in characterising the thermal history of dolomite hydrocarbon reservoirs. It
413 may be particularly useful to help distinguish early-shallow from deep-burial origin of dolomite
414 formations.

415

416 Acknowledgements

417

418 Annabel Dale, Tobias Kluge and Simon Davis are thanked for assistance in the Qatar Stable Isotope
419 Lab at Imperial College London. Two grants awarded to CJ from TOTAL E&P (# 4200059621 and
420 4300002831) enabled this work to be carried out. Ethan Grossman and an anonymous reviewer are
421 thanked for their reviews which considerably improved the manuscript and Mike Lawson is thanked
422 for editorial handling.

423

424 Figure Captions

425

426 Figure 1: (a) map showing the general location of the studied samples, offshore Angola, after
427 Eichenseer et al., (1999); (b) burial history of the Pinda Formation.

428

429 Figure 2: Fluid inclusion temperatures for the Pinda Formation (data reproduced from Eichenseer et
430 al., 1999). Fluid inclusion homogenisation temperatures shown as red squares represent sample
431 averages, while horizontal black bars represent the range of individual T_h values. Current ambient
432 well temperatures are shown as blue diamonds, and are in close concordance with T_h average values
433 (with one exception at ~3 km depth).

434

435 Figure 3: Plane polarized light photomicrographs showing typical petrographic textures of samples
436 from the Pinda Formation. (a) blocky planar-s dolosparite texture typical of many of the samples,
437 arrow denotes example of a sand grain; (b) red staining indicating minor calcite component, arrow
438 denotes example of preserved ooid fabric typical of many of the samples; (c) moldic pore after ooid,
439 lined with small euhedral dolomite rhombs; (d) rare preserved shell fabric.

440

441 Figure 4: Isotope data and Δ_{47} -derived temperatures for the seven samples from the Pinda
442 Formation analysed for clumped isotopes, plotted against sample depth. (a) $\delta^{13}\text{C}$; (b) $\delta^{18}\text{O}$; (c)
443 clumped isotope, fluid inclusion and ambient well temperatures; (d) parent fluid $\delta^{18}\text{O}$, shaded areas
444 represent typical source fluid values.

445

446 Figure 5: ‘Worst case’ scenario of post-depositional evolution of Δ_{47} values in the Pinda Formation,
447 assuming the samples were calcite not dolomite. Modelled in the style of Shenton et al., (2015)
448 using the calcite reordering kinetics of Passey and Henkes (2012) for optical calcite MGB-CC-1. (a)

449 the base Pinda, based on an extrapolation of the ‘representative’ Pinda burial history modelled by
450 TOTAL shown in (b).

451

452 Table Captions

453

454 Table 1: Summary table of sample details, isotopic values and temperatures. CDES denotes Carbon
455 Dioxide Equilibration Scale (Dennis, et al., 2011); T_h denotes fluid inclusion homogenisation
456 temperature (sample average); T_{well} denotes current ambient well temperature; T_{cl} denotes
457 clumped isotope temperature.

458

459 References

460

461 Affek, H. P., Bar-Matthews, M., Ayalon, A., Matthews, A. & Eiler, J. M., 2008. Glacial/interglacial
462 temperature variations in Soreq cave speleothems as recorded by ‘clumped isotope’
463 thermometry. *Geochimica et Cosmochimica Acta*, **72**(22), 5351-5360.

464 Barker, C. E. & Goldstein, R. H., 1990. Fluid-inclusion technique for determining maximum
465 temperature in calcite and its comparison to the vitrinite reflectance geothermometer.
466 *Geology*, **18**(10), 1003-1006.

467 Bonifacie, M., Calmels, D. & Eiler, J., 2013. Clumped isotope thermometry of marbles as an indicator
468 of the closure temperatures of calcite and dolomite with respect to solid-state reordering of
469 C–O bonds. In: *Goldschmidt 2013*, Mineralogical Magazine, Florence.

470 Bremner, A. N., Lomando, A. J. & Minck, R. J., 1993. Successful Exploration of the Outer Pinda Trend
471 of Offshore Cabinda, Angola. In: *AAPG International Conference and Exhibition*, The Hague.

472 Carrapa, B., Huntington, K. W., Clementz, M., Quade, J., Bywater-Reyes, S., Schoenbohm, L. M. &
473 Canavan, R. R., 2014. Uplift of the Central Andes of NW Argentina associated with upper
474 crustal shortening, revealed by multiproxy isotopic analyses. *Tectonics*, **33**(6), 1039-1054.

475 Coajou, A. & Ribeiro, A., 1994. Angola Block 3 - from Wildcat to Intensive Exploration 22 Discoveries -
476 1 Billion BBL Recoverable Oil. In: *14th World Petroleum Congress*, Stavanger.

477 Dale, A., John, C. M., Mozley, P. S., Smalley, P. C. & Muggeridge, A. H., 2014. Time-capsule
478 concretions: Unlocking burial diagenetic processes in the Mancos Shale using carbonate
479 clumped isotopes. *Earth and Planetary Science Letters*, **394**, 30-37.

480 Dennis, K. J., Affek, H. P., Passey, B. H., Schrag, D. P. & Eiler, J. M., 2011. Defining an absolute
481 reference frame for ‘clumped’ isotope studies of CO₂. *Geochimica et Cosmochimica Acta*,
482 **75**(22), 7117-7131.

483 Dennis, K. J. & Schrag, D. P., 2010. Clumped isotope thermometry of carbonatites as an indicator of
484 diagenetic alteration. *Geochimica et Cosmochimica Acta*, **74**(14), 4110-4122.

485 Eichenseer, H. T., Walgenwitz, F. R. & Biondi, P. J., 1999. Stratigraphic control on facies and
486 diagenesis of dolomitized oolitic siliciclastic ramp sequences (Pinda group, Albian, offshore
487 Angola). *Aapg Bulletin-American Association of Petroleum Geologists*, **83**(11), 1729-1758.

488 Eiler, J. M., 2007. “Clumped-isotope” geochemistry—The study of naturally-occurring, multiply-
489 substituted isotopologues. *Earth and Planetary Science Letters*, **262**(3-4), 309-327.

490 Emiliani, C., 1955. Pleistocene Temperatures. *The Journal of Geology*, **63**(6), 538-578.

491 Epstein, S., Buchsbaum, R., Lowenstam, H. & Urey, H., 1951. Carbonate-Water Isotopic Temperature
492 Scale. *Bulletin Of The Geological Society Of America*, **62**, 417-426.

493 Ferry, J. M., Passey, B. H., Vasconcelos, C. & Eiler, J. M., 2011. Formation of dolomite at 40-80 °C in
494 the Latemar carbonate buildup, Dolomites, Italy, from clumped isotope thermometry.
495 *Geology*, **39**(6), 571-574.

496 Geske, A., Goldstein, R. H., Mavromatis, D. K., Richter, D. K., Buhl, D., Kluge, T., John, C. M. &
497 Immenhauser, A., 2015. The magnesium isotope ($\delta^{26}\text{Mg}$) signature of dolomites.
498 *Geochimica et Cosmochimica Acta*, **149**, 131-151.

- 499 Ghosh, P., Adkins, J., Affek, H., Balta, B., Guo, W., Schauble, E. A., Schrag, D. & Eiler, J. M., 2006a.
500 13C–18O bonds in carbonate minerals: A new kind of paleothermometer. *Geochimica et*
501 *Cosmochimica Acta*, **70**(6), 1439-1456.
- 502 Ghosh, P., Garzione, C. N. & Eiler, J. M., 2006b. Rapid uplift of the Altiplano revealed through C-13-O-
503 18 bonds in paleosol carbonates. *Science*, **311**(5760), 511-515.
- 504 Goldstein, R. H., 2001. Fluid inclusions in sedimentary and diagenetic systems. *Lithos*, **55**(1–4), 159-
505 193.
- 506 Goldstein, R. H. & Reynolds, T. J., 1994. *Systematics of fluid inclusions in diagenetic minerals*. Society
507 for Sedimentary Geology.
- 508 Guo, W., Mosenfelder, J. L., Goddard, W. A. & Eiler, J. M., 2009. Isotopic fractionations associated
509 with phosphoric acid digestion of carbonate minerals: Insights from first-principles
510 theoretical modeling and clumped isotope measurements. *Geochimica et Cosmochimica*
511 *Acta*, **73**(24), 7203-7225.
- 512 Henkes, G. A., Passey, B. H., Grossman, E. L., Shenton, B. J., Perez-Huerta, A. & Yancey, T. E., 2014.
513 Temperature limits for preservation of primary calcite clumped isotope paleotemperatures.
514 *Geochimica Et Cosmochimica Acta*, **139**, 362-382.
- 515 Hu, B., Radke, J., Schlüter, H.-J., Heine, F. T., Zhou, L. & Bernasconi, S. M., 2014. A modified
516 procedure for gas-source isotope ratio mass spectrometry: the long-integration dual-inlet
517 (LIDI) methodology and implications for clumped isotope measurements. *Rapid*
518 *Communications in Mass Spectrometry*, **28**(13), 1413-1425.
- 519 Huntington, K. W., Eiler, J. M., Affek, H. P., Guo, W., Bonifacie, M., Yeung, L. Y., Thiagarajan, N.,
520 Passey, B., Tripathi, A., Daeron, M. & Came, R., 2009. Methods and limitations of 'clumped'
521 CO₂ isotope (Delta47) analysis by gas-source isotope ratio mass spectrometry. *Journal of*
522 *mass spectrometry : JMS*, **44**(9), 1318-29.
- 523 Huntington, K. W., Wernicke, B. P. & Eiler, J. M., 2010. Influence of climate change and uplift on
524 Colorado Plateau paleotemperatures from carbonate clumped isotope thermometry.
525 *Tectonics*, **29**, 19.
- 526 John, C. M., 2015. Burial Estimates Constrained by Clumped Isotope thermometry: Example of the
527 Lower Cretaceous Qishn Formation (Haushi-Huqf high, Oman).
- 528 Kluge, T. & John, C. M., 2015. Effects of brine chemistry and polymorphism on clumped isotopes
529 revealed by laboratory precipitation of mono- and multiphase calcium carbonates.
530 *Geochimica et Cosmochimica Acta*, **160**(0), 155-168.
- 531 Kluge, T., John, C. M., Jourdan, A. L., Davis, S. & Crawshaw, J., 2015. Laboratory calibration of the
532 calcium carbonate clumped isotope thermometer in the 25-250°C temperature range.
533 *Geochimica et Cosmochimica Acta*, **In Press**.
- 534 Koutsoukos, E. A. M., Mello, M. R., Filho, N. C. D., Hart, M. B. & Maxwell, J. R., 1991. The Upper
535 Aptian Albian Succession of the Sergipe Basin, Brazil - an Integrated Paleoenvironmental
536 Assessment. *Aapg Bulletin-American Association of Petroleum Geologists*, **75**(3), 479-498.
- 537 Land, L. S., 1980. The isotopic and trace element geochemistry of dolomite: The state of the art. In:
538 *Concepts of models of dolomitization* (eds Zenger, D. H., Dunham, D. W. & L., E. R.), pp. 87-
539 110, Society of Economic Paleontologists and Mineralogists Special Publication.
- 540 Lechler, A. R., Niemi, N. A., Hren, M. T. & Lohmann, K. C., 2013. Paleoelevation estimates for the
541 northern and central proto-Basin and Range from carbonate clumped isotope thermometry.
542 *Tectonics*, **32**(3), 295-316.
- 543 MacDonald, J., John, C. & Girard, J.-P., 2015. Dolomitization Processes in Hydrocarbon Reservoirs:
544 Insight from Geothermometry Using Clumped Isotopes. *Procedia Earth and Planetary*
545 *Science*, **13**, 265-268.
- 546 MacDonald, J. M., John, C. M. & Girard, J.-P., 2013. Application of clumped isotope thermometry to
547 subsurface dolostone samples. In: *Goldschmidt 2013*, pp. 1662, Mineralogical Magazine,
548 Florence.

- 549 McCrea, J. M., 1950. On the Isotopic Chemistry of Carbonates and a Paleotemperature Scale. *The*
550 *Journal of Chemical Physics*, **18**(6), 849-857.
- 551 McLimans, R. K., 1987. The application of fluid inclusions to migration of oil and diagenesis in
552 petroleum reservoirs. *Applied Geochemistry*, **2**(5-6), 585-603.
- 553 Meckler, A. N., Ziegler, M., Millan, M. I., Breitenbach, S. F. & Bernasconi, S. M., 2014. Long-term
554 performance of the Kiel carbonate device with a new correction scheme for clumped isotope
555 measurements. *Rapid Commun Mass Spectrom*, **28**(15), 1705-15.
- 556 Nadeau, P. H., 2011. Earth's energy "Golden Zone": a synthesis from mineralogical research. *Clay*
557 *Minerals*, **46**, 1-24.
- 558 Passey, B. H. & Henkes, G. A., 2012. Carbonate clumped isotope bond reordering and
559 geospeedometry. *Earth and Planetary Science Letters*, **351-352**, 223-236.
- 560 Passey, B. H., Levin, N. E., Cerling, T. E., Brown, F. H. & Eiler, J. M., 2010. High-temperature
561 environments of human evolution in East Africa based on bond ordering in paleosol
562 carbonates. *Proceedings of the National Academy of Sciences of the United States of*
563 *America*, **107**(25), 11245-9.
- 564 Petersen, S. V. & Schrag, D. P., 2014. Clumped isotope measurements of small carbonate samples
565 using a high-efficiency dual-reservoir technique. *Rapid Communications in Mass*
566 *Spectrometry*, **28**(21), 2371-2381.
- 567 Reyre, D., 1984. Caracteres petroliers et evolution geologique d' une marge passive. Le cas du Bassin
568 Bas Congo-Gabon. *Bulletin du Centre de Recherche Exploration-Production Elf-Aquitaine*,
569 **8**(2), 303-332.
- 570 Rosenbaum, J. & Sheppard, S. M. F., 1986. An Isotopic Study of Siderites, Dolomites and Ankerites at
571 High-Temperatures. *Geochimica Et Cosmochimica Acta*, **50**(6), 1147-1150.
- 572 Schauble, E. A., Ghosh, P. & Eiler, J. M., 2006. Preferential formation of ¹³C-¹⁸O bonds in carbonate
573 minerals, estimated using first-principles lattice dynamics. *Geochimica et Cosmochimica*
574 *Acta*, **70**(10), 2510-2529.
- 575 Sena, C. M., John, C. M., Jourdan, A. L., Vandeginste, V. & Manning, C., 2014. Dolomitization of
576 Lower Cretaceous Peritidal Carbonates by Modified Seawater: Constraints from Clumped
577 Isotopic Paleothermometry, Elemental Chemistry, and Strontium Isotopes. *Journal of*
578 *Sedimentary Research*, **84**(7), 552-566.
- 579 Shackleton, N., 1967. Oxygen Isotope Analyses and Pleistocene Temperatures Re-assessed. *Nature*,
580 **215**(5096), 15-17.
- 581 Shenton, B. J., Grossman, E. L., Passey, B. H., Henkes, G. A., Becker, T. P., Laya, J. C., Perez-Huerta, A.,
582 Becker, S. P. & Lawson, M., 2015. Clumped isotope thermometry in deeply buried
583 sedimentary carbonates: The effects of bond reordering and recrystallisation. *GSA Bulletin*,
584 **127**.
- 585 Sibley, D. F. & Gregg, J. M., 1987. Classification of Dolomite Rock Textures. *Journal of Sedimentary*
586 *Petrology*, **57**(6), 967-975.
- 587 Stolper, D. & Eiler, J., 2016. Constraints on the formation and diagenesis of phosphorites using
588 carbonate clumped isotopes. *Geochimica et Cosmochimica Acta*, **181**, 238-259.
- 589 Stolper, D. A. & Eiler, J. M., 2015. The kinetics of solid-state isotope-exchange reactions for clumped
590 isotopes: A study of inorganic calcites and apatites from natural and experimental samples.
591 *American Journal of Science*, **315**(5), 363-411.
- 592 Thiagarajan, N., Subhas, A. V., Southon, J. R., Eiler, J. M. & Adkins, J. F., 2014. Abrupt pre-Bolling-
593 Allerod warming and circulation changes in the deep ocean. *Nature*, **511**(7507), 75-U409.
- 594 Urey, H. C., Lowenstam, H. A., Epstein, S. & Mckinney, C. R., 1951. Measurement Of
595 Paleotemperatures And Temperatures Of The Upper Cretaceous Of England, Denmark, And
596 The Southeastern United States. *Geological Society of America Bulletin*, **62**(4), 399-416.
- 597 Vandeginste, V., John, C. M., Cosgrove, J. W. & Manning, C., 2014. Dimensions, texture-distribution,
598 and geochemical heterogeneities of fracture- related dolomite geobodies hosted in
599 Ediacaran limestones, northern Oman. *Aapg Bulletin*, **98**(9), 1789-1809.

600 Veizer, J., Ala, D., Azmy, K., Bruckschen, P., Buhl, D., Bruhn, F., Carden, G. A. F., Diener, A., Ebner, S.,
601 Godderis, Y., Jasper, T., Korte, C., Pawellek, F., Podlaha, O. G. & Strauss, H., 1999. Sr-87/Sr-
602 86, delta C-13 and delta O-18 evolution of Phanerozoic seawater. *Chemical Geology*, **161**(1-
603 3), 59-88.

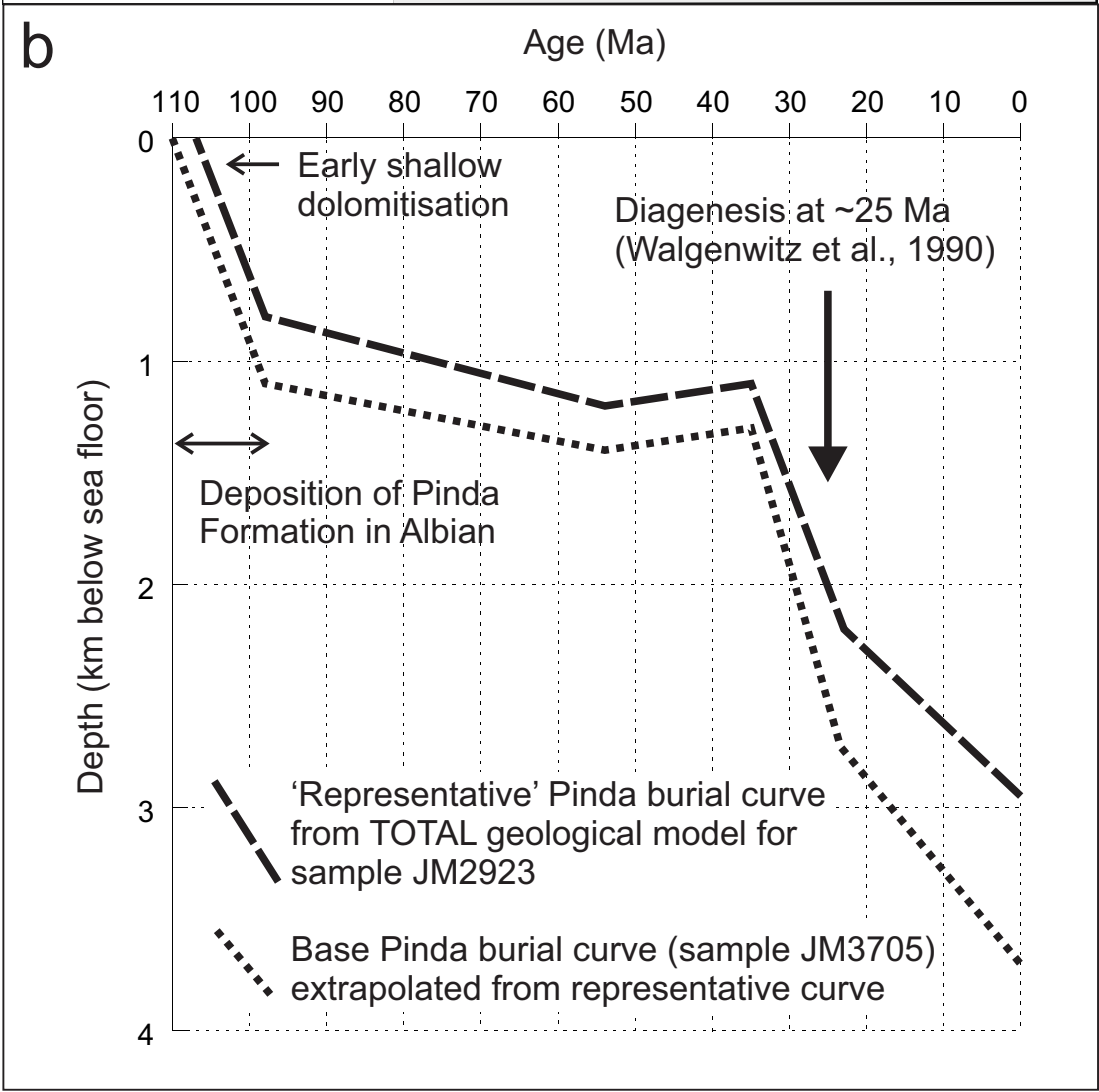
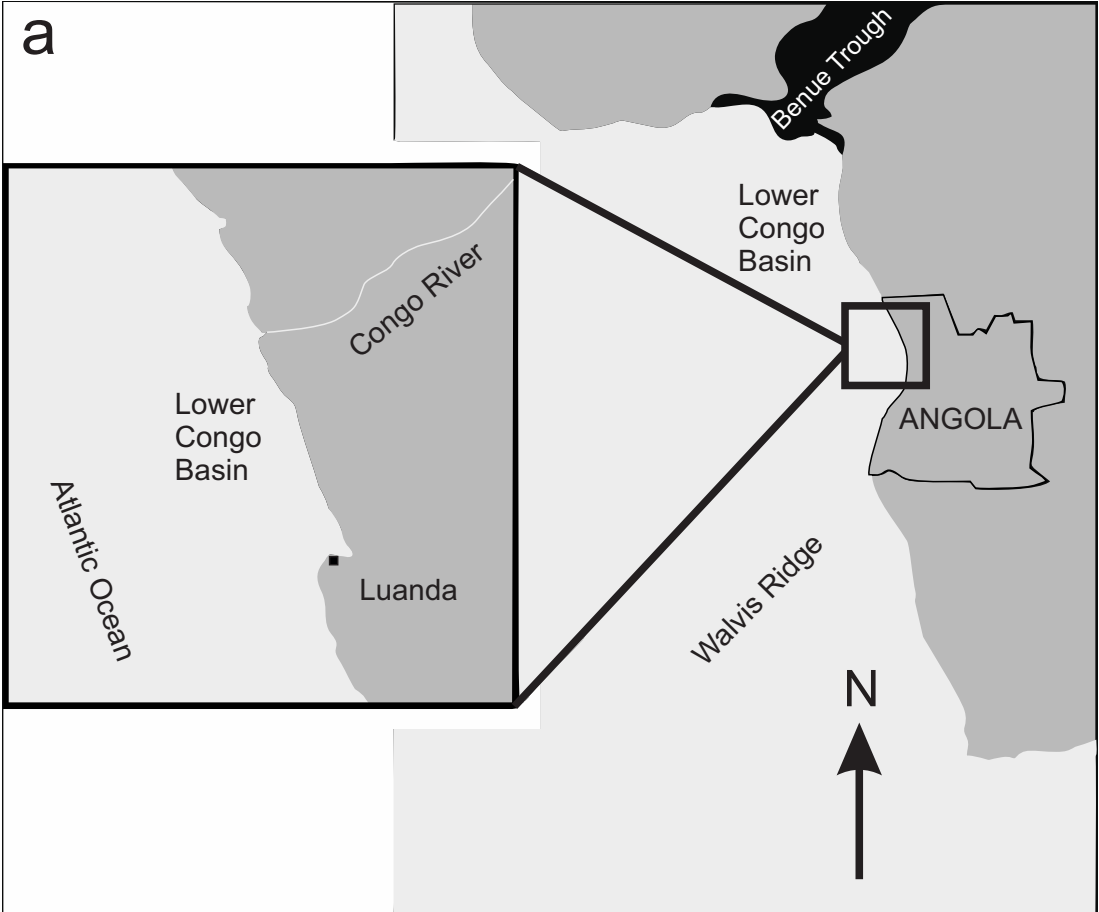
604 Wacker, U., Fiebig, J. & Schoene, B. R., 2013. Clumped isotope analysis of carbonates: comparison of
605 two different acid digestion techniques. *Rapid Commun Mass Spectrom*, **27**(14), 1631-42.

606 Walgenwitz, F., 1989. CACO 2 (Angola) Etude de la diagenèse et des inclusions fluides du reservoir
607 Pinda, carottes 1 à 3. In: *Total internal report, EP/EXP/Lab*, Pau N°89/2055 RP.

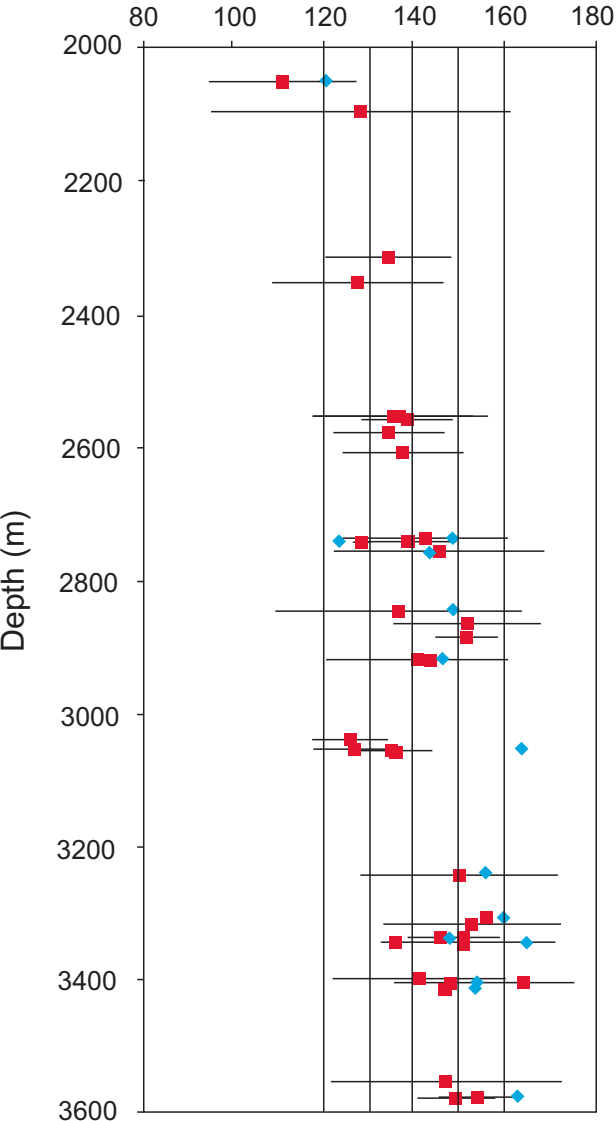
608 Walgenwitz, F., Pagel, M., Meyer, A., Maluski, H. & Monie, P., 1990. Thermochronological Approach
609 to Reservoir Diagenesis in the Offshore Angola Basin - a Fluid Inclusion, Ar-40-Ar-39 and K-Ar
610 Investigation. *Aapg Bulletin-American Association of Petroleum Geologists*, **74**(5), 547-563.

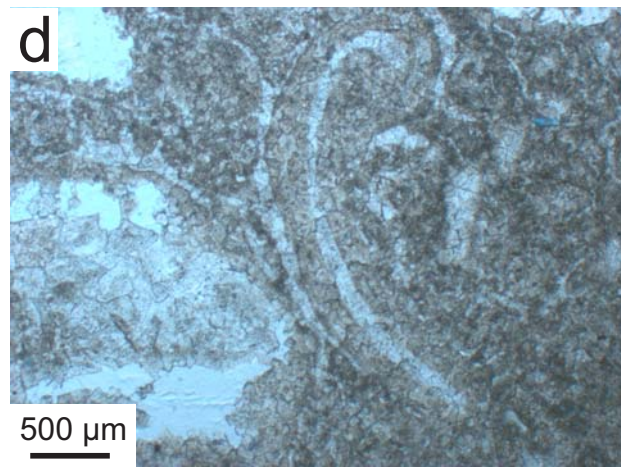
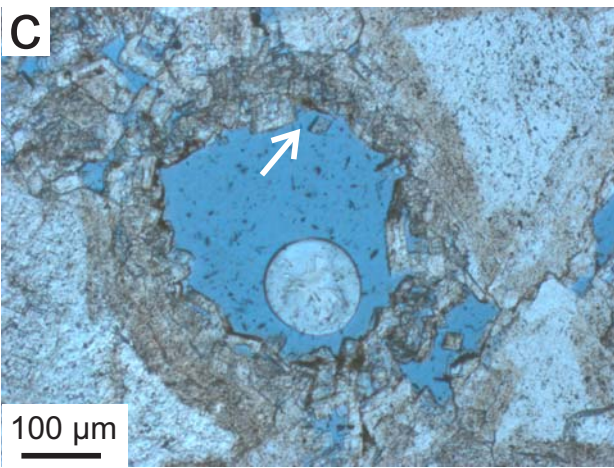
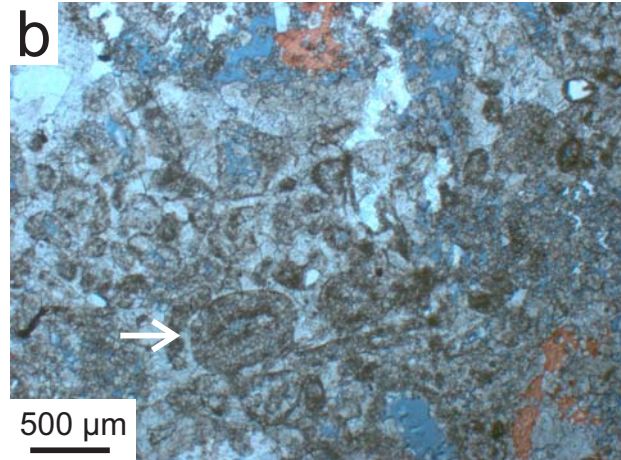
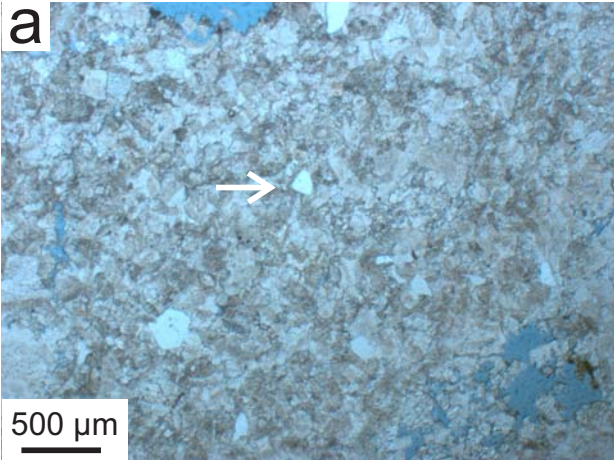
611

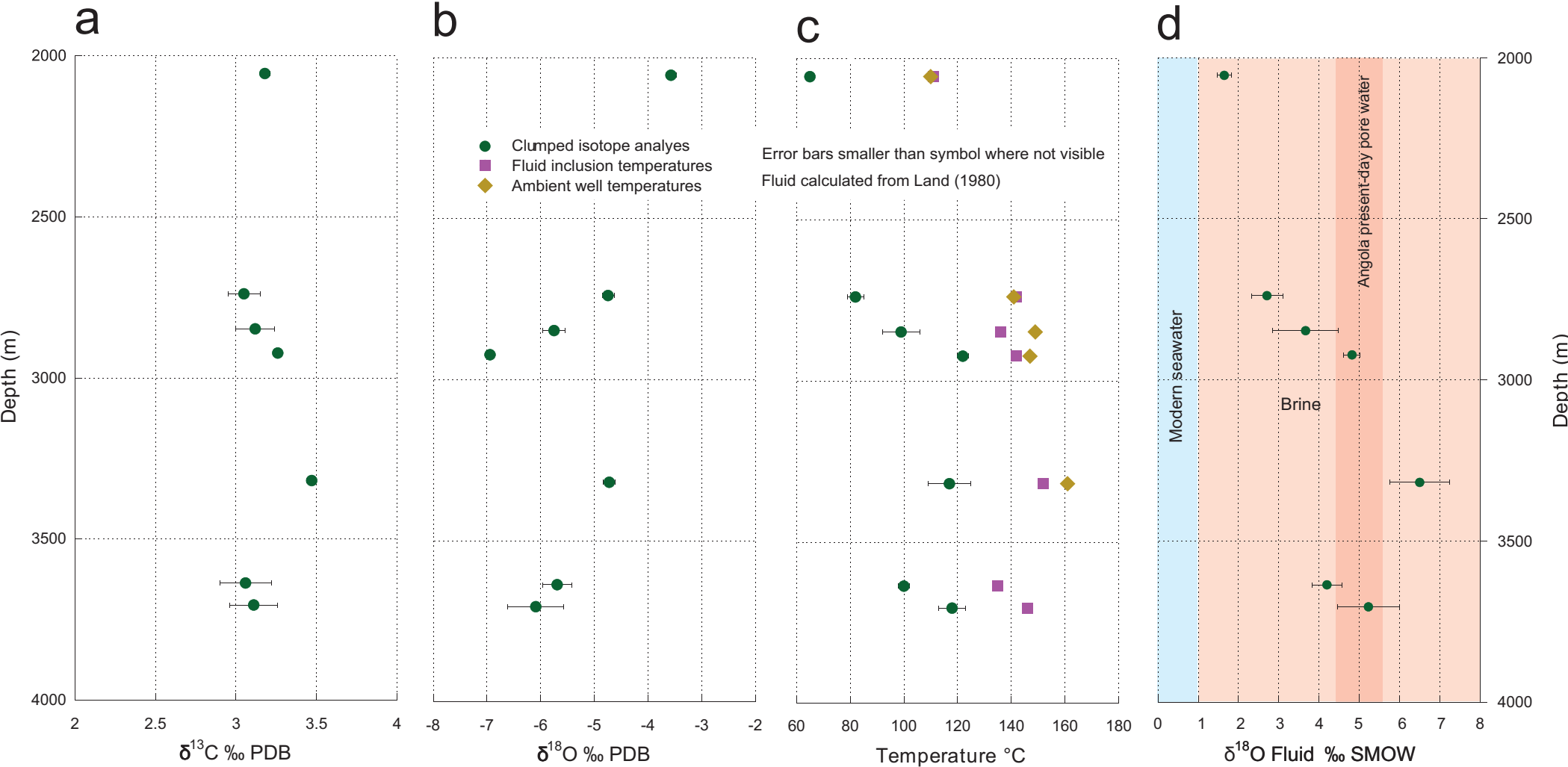
Sample	Depth (m)	No. of Analyses	Mineral $\delta^{13}\text{C}$ (‰) PDB	StDev (‰)	Mineral $\delta^{18}\text{O}$ (‰) PDB	StDev (‰)	Δ_{47} CDES (‰)	StErr (‰)	T_h (°C)	T_{well} (°C)	$T(\Delta_{47})$ (°C)	StErr (°C)	Fluid $\delta^{18}\text{O}$ (‰) SMOW	StErr (‰)
JM2055	2055	3	3.18	0.03	-3.57	0.10	0.592	0.001	111	110	65	1	1.7	0.2
JM2740	2740	3	3.05	0.10	-4.74	0.11	0.560	0.005	142	141	82	3	2.7	0.4
JM2848	2848	5	3.12	0.12	-5.75	0.21	0.530	0.011	136	149	99	5	3.7	0.8
JM2923	2923	3	3.26	0.01	-6.94	0.03	0.495	0.003	142	147	122	1	4.8	0.2
JM3319	3319	3	3.47	0.03	-4.72	0.11	0.503	0.010	152	161	117	6	6.5	0.8
JM3637	3637	5	3.06	0.16	-5.69	0.27	0.528	0.004	135	n/a	100	2	4.2	0.4
JM3705	3705	3	3.11	0.15	-6.09	0.52	0.502	0.008	146	n/a	118	7	5.2	0.8

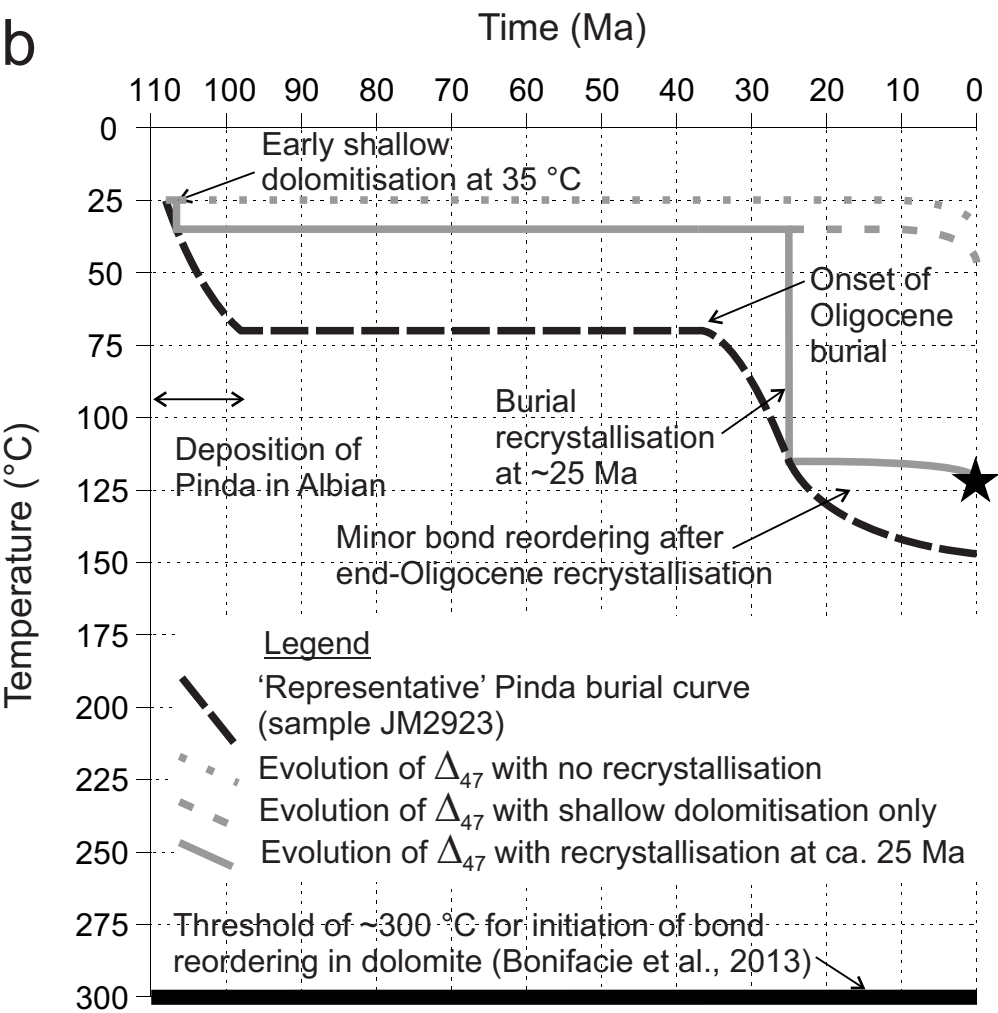
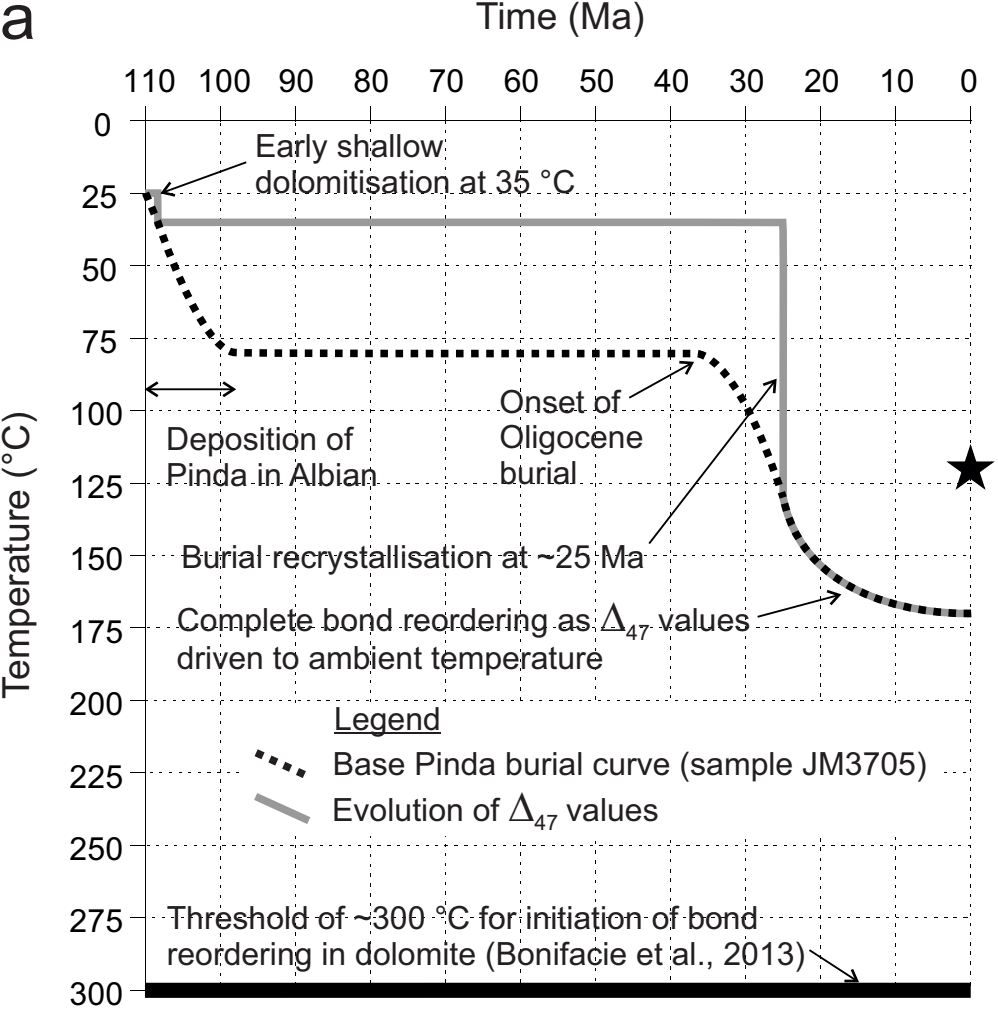


Temperature (°C)









★ denotes measured clumped isotope temperature